PHYSICS AND CHEMISTRY OF SOLID STATE
V. 23, No. 4 (2022) pp. 699-704
Section: Chemistry

DOI: 10.15330/pcss.23.4.699-704

Vasyl Stefanyk Precarpathian National University

ФІЗИКА І ХІМІЯ ТВЕРДОГО ТІЛА
Т. 23, № 4 (2022) С. 699-704
Хімічні науки

UDC: 621.355 ISSN 1729-4428

V. Kordan[1], O. Zaremba[1], P. Demchenko[1], V. Pavlyuk[1,2]

Synthesis and electrochemical properties of $Li_yM_{1-x}Ca_xMnO_3$ (M = Pr, Eu) solid solutions

[1]*Ivan Franko National University of Lviv, Lviv, Ukraine,*
[2]*Jan Długosz University of Czestochowa, Czestochowa, Poland,* vasyl.kordan@lnu.edu.ua

New Li-containing solid solutions $Li_yM_{1-x}Ca_xMnO_3$ (M = Pr and Eu) were synthesized by electrochemical lithiation of the ceramics with perovskite structure. The qualitative and quantitative composition of the initial and Li-containing ceramics was determined by scanning electron microscopy and energy-dispersive X-ray spectroscopy. The M/Ca/Mn cation ratio was confirmed by X-ray fluorescence spectroscopy. The crystal structure of the$M_{1-x}Ca_xMnO_3$solid solutions before lithiation ($GdFeO_3$-type structure, space group *Pnma*, Pearson code *oP*20) and after lithiation (filled-up $GdFeO_3$-type) was determined by the Rietveld method. X-ray structural analysis showed the formation of phases with increased unit cell parameters after lithiation process. In the case of Eu and Pr-containing samples X-rays diffraction patterns illustrate the amorphous halo based on the by-products of reaction between of ceramics surface and components from electrolyte. Under experimental conditions (Li-metal anode) the quantity of intercalated Li increases for ceramics: $Li_{0.084}Eu_{0.5}Ca_{0.5}MnO_3$, $Li_{0.113}Pr_{0.5}Ca_{0.5}MnO_3$, and $Li_{0.134}Pr_{0.7}Ca_{0.3}MnO_3$. Scanning electron microscopy method revealed the formation of Li-containing aggregates with dimension of 200-900 nm. The grains demonstrate block-like or irregular shape morphology with developed area surface.

Keywords: X-ray diffraction; electron microscopy; perovskite structure; electrochemical lithiation.

Received 09 August2022; Accepted 04 November 2022.

Introduction

Complex ceramics as well as intermetallic compounds are widely used as thebasis of modern materials with multifunctional properties. For today the synthesis of nano-multicomponent substances and the investigation of influence of different doping components on their crystal structures and physicochemical properties is one of the most popular trends in many fields of science [1]. Perovskites, spinels and garnets are among the highest promising materials for technology, including energy industry, such as the mixed oxidation state of their components is often the cause of unique physical properties. Magnetic, photoelectric (energy accumulation), catalytic properties, the characterizationas electrodes in solid oxide fuel cell (energy transformation) are the best studied [1-12]. Perovskites with variable oxidation state of elements (Mn^{2+}/Mn^{3+}, Mn^{3+}/Mn^{4+}, Pr^{3+}/Pr^{4+}, Eu^{2+}/Eu^{3+}, V^{4+}/V^{5+}, Pb^{2+}/Pb^{4+} etc.) and cation defects in the crystal structure seem to be specially interesting for scientists, engineers, and inventors as prospective cathode materials. The improvement of corrosion resistance, thermal stability and increasing of discharge capacity of cathodes can operate using Li-doping of electrodes [13]. In our previous works we have studied the influence of doping components on electrochemical properties of intermetallic compounds or solid solutions as electrode materials [14-18]. Ternary intermetallics from systems of rare-earth metals, transition metals and magnesium (zinc or cadmium) [19-22] are considered especially promising, where, in addition to insertion, the replacement of electrochemically active elements (Mg, Zn or Cd) by lithium may takes place. The aim of this work was to synthesize the $Li_yM_{1-x}Ca_xMnO_3$ (M = Pr, Eu) ceramics and investigate its electrochemical properties as cathode material in Li-ion prototype battery.

I. Materials and experimental methods

Initial $M_{1-x}Ca_xMnO_3$ (M = Pr, Eu) ceramic samples were synthesized by two-stage solid-state reaction method starting from appropriate quantities of oxides and carbonates of high purity. At the beginning the reagents were mixed manually and heated in the muffle furnace at 1000°C during 24 hours. Then the mixtures were ground, pressed and sintered in the tube furnace at 1200°C during 8 hours. Electrochemical lithiation was investigated in a two-electrode Swagelok-type cell. A synthesized powdered ceramics was used as cathode material. It was mixed with the electrolyte (1M Li[PF_6] solution in 1:1 ethylenecarbonate/dimethylcarbonate). As anode we used the sheet of Li-metal (99.8 wt.%, commercial). Electrochemical measurements were carried out in the galvanostatic mode at 0.2 mA/cm^2 using MTech G410-2 galvanostat [23]. The amount of Li per formula unit (Li/f.u.) was determined for studied electrodes using Faraday's formula, where Li-content is directly proportional to the discharge time. The electrochemical reactions that occur in the case of $Pr_{0.5}Ca_{0.5}MnO_3$ ceramics as cathode can be presented by the following scheme:

$$\text{Cathode: } Pr_{0.5}Ca_{0.5}MnO_3 + yLi^+ + y\bar{e} \underset{\text{charge (delithiation)}}{\overset{\text{discharge (lithiation)}}{\rightleftharpoons}} Li_yPr_{0.5}Ca_{0.5}MnO_3$$

$$\text{Anode: } Li \underset{\text{charge (delithiation)}}{\overset{\text{discharge (lithiation)}}{\rightleftharpoons}} yLi^+ + y\bar{e}$$

In the case of Eu, we can see two reactions. Besides lithiation as targeted electrochemical reaction we assume the redox by-reaction of Eu^{2+}/Eu^{3+} transformation.

Diffraction data before and after electrochemical lithiation were collected on STOE STADI P automatic powder diffractometer (Cu $K_{\alpha 1}$-radiation, Ge111-monochromator). The experimental diffraction patterns of samples were compared with the theoretical ones, structural analysis was performed by Rietveld refinement using the FullProf program [24]. The qualitative and quantitative compositions of studied samples were established applying energy-dispersive X-ray spectroscopy (Tescan Vega 3 LMU scanning electron microscope with Oxford Instruments AZtec ONE System). SEM and energy-dispersive X-ray analysis (EDX) were performed at 21–25 kV voltage and high vacuum atmosphere. X-ray fluorescence spectroscopy was used for determination M/Ca/Mn ratio (ElvaX Pro X-ray fluorescence analyzer).

II. Results and discussion

X-ray phase and structural analysis of the synthesized complex oxides $M_{1-x}Ca_xMnO_3$(M = Pr, Eu) showed the presence of phases with orthorhombic $GdFeO_3$-type structure only (space group *Pnma*, Pearson code *oP*20). The unit cell parameters of these phases correlate well with the cation radius of the rare-earth metal: $r(Ca^{2+})$ = 0.94 Å, $r(Eu^{3+})$ = 0.96 Å, and$r(Pr^{3+})$ = 1.01 Å. We observed an increase of cell volume with increasing of praseodymium content. Rietveld refinement showed that R-factors for Li-containing samples were some what higher due to partial amorphization and formation of by-products after lithiation. After lithiation the unit cell parameters are increased (Table 1). XRD powder patterns of $M_{1-x}Ca_xMnO_3$ (M = Pr, Eu) samples before and after lithiation are presented at Fig. 1. For Eu-containing sample after lithiation the small amounts of unidentified phases with low intensity peaks were observed simultaneously with amorphous halo at small

Table 1

Cell parameters of ceramics before and after lithiation.

Initial	Lithiated	$\Delta V/V$, %
$Eu_{0.5}Ca_{0.5}MnO_3$ a = 5.3904(12) Å, b = 7.523(2) Å, c = 5.3379(12) Å, V = 216.48(9) Å^3; R_B = 0.0996, R_p = 0.0309, R_{wp} = 0.0386	**$Li_xEu_{0.5}Ca_{0.5}MnO_3$** a = 5.4015(11) Å, b = 7.5259(18) Å, c = 5.3442(11) Å, V = 217.25(8)Å^3; trace amounts of by-products of lithiation; R_B = 0.107, R_p = 0.0295, R_{wp} = 0.0373	0.36
$Pr_{0.5}Ca_{0.5}MnO_3$ a = 5.3848(7) Å, b = 7.5976(8) Å, c = 5.3996(6) Å, V = 220.91(4) Å^3; R_B = 0.0614, R_p = 0.0338, R_{wp} = 0.0426	**$Li_xPr_{0.5}Ca_{0.5}MnO_3$** a = 5.3894(11) Å, b = 7.6036(13) Å, c = 5.4046(9) Å, V = 221.48(7) Å^3; R_B = 0.0749, R_p = 0.0427, R_{wp} = 0.0539	0.26
$Pr_{0.7}Ca_{0.3}MnO_3$ a = 5.4387(12) Å, b = 7.7107(16) Å, c = 5.4070(10) Å, V = 226.75(8) Å^3; R_B = 0.0740, R_p = 0.0367, R_{wp} = 0.0461	**$Li_xPr_{0.7}Ca_{0.3}MnO_3$** a = 5.4418(19) Å, b = 7.720(3) Å, c = 5.4046(16) Å, V = 227.05(13) Å^3; trace amount **oxidized Li-containing phases**; R_B = 0.123, R_p = 0.0668, R_{wp} = 0.0851	0.13

angel area (5-30° 2θ). New phases are crystallized by interaction of the oxide surface and components from the electrolyte.

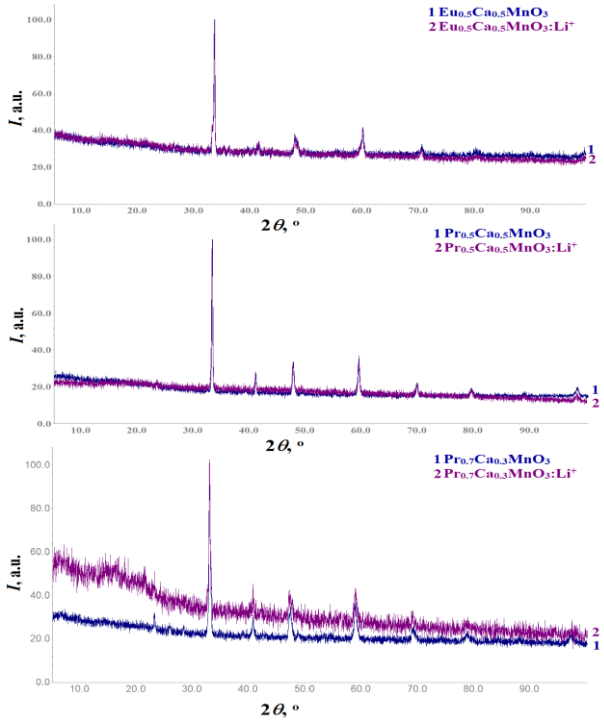

Fig. 1. XRD powder patterns of $M_{1-x}Ca_xMnO_3$ (M = Pr, Eu) samples before (1) and after lithiation (2).

The change of $Eu_{0.5}Ca_{0.5}MnO_3$ ceramics morphology after lithiation is shown at Fig. 2. One can easily see the aggregation of Li-based particles with the formation of spherical-type grains up to 1000 nm. In the case of lithiated $Pr_{1-x}Ca_xMnO_3$ solid solutions we observed the block-like or irregular-type particles (Fig. 3, 4). Small aggregates or blocks have dimension of 200-600 nm. $Li_xPr_{0.7}Ca_{0.3}MnO_3$ sample oxidizes quite quickly in air. Also this sample demonstrates considerable amorphous halo. Lithium-containing phases are easily hydrolyzed with the formation of intermediate amorphous compounds.

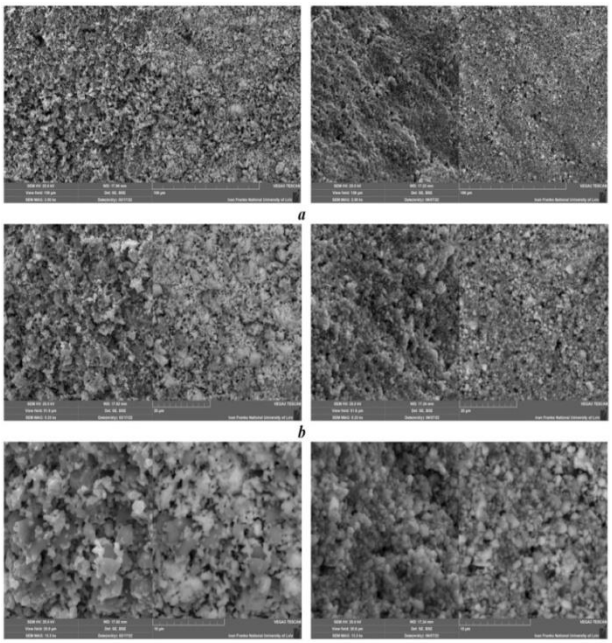

Fig. 2. SEM-images of $Eu_{0.5}Ca_{0.5}MnO_3$ before (left) and after (right) lithiation at different magnification: a – 2000x, b – 5330x, c – 13300x.

The integral composition (cation ratio M/Ca/Mn) of studied ceramics was confirmed by X-ray fluorescent spectroscopy. Also, the composition from energy-dispersive X-ray spectroscopy correlates well with the nominal composition of the samples. After lithiation the composition of cathode materials are $Eu_{7.4}Ca_{10.4}Mn_{21.9}O_{60.3}$, $Pr_{8.7}Ca_{9.4}Mn_{18.8}O_{63.1}$, and $Pr_{14.9}Ca_{5.8}Mn_{20.2}O_{59.1}$. Elemental mapping demonstrates homogenous component distribution on the grain surface.

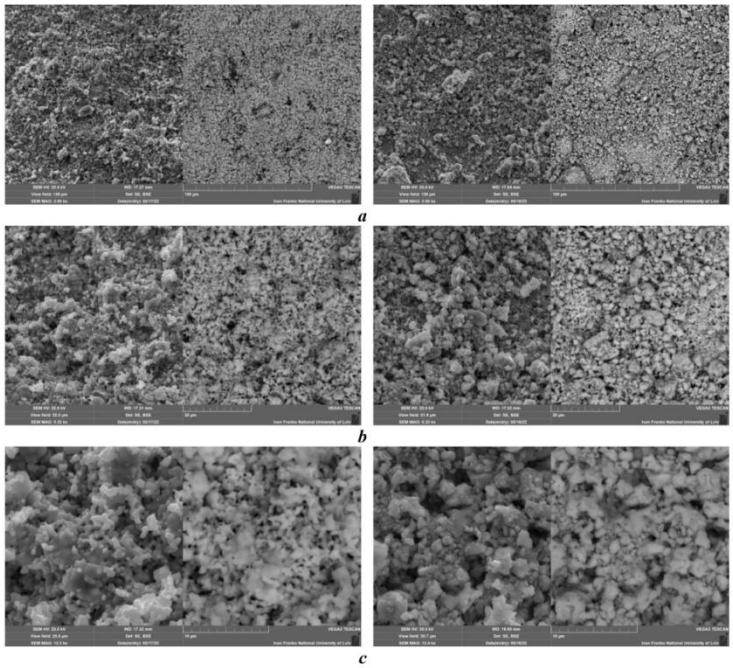

Fig. 3. SEM-images of $Pr_{0.5}Ca_{0.5}MnO_3$ before (left) and after (right) lithiation at different magnification: a – 2000x, b – 5330x, c – 13300x

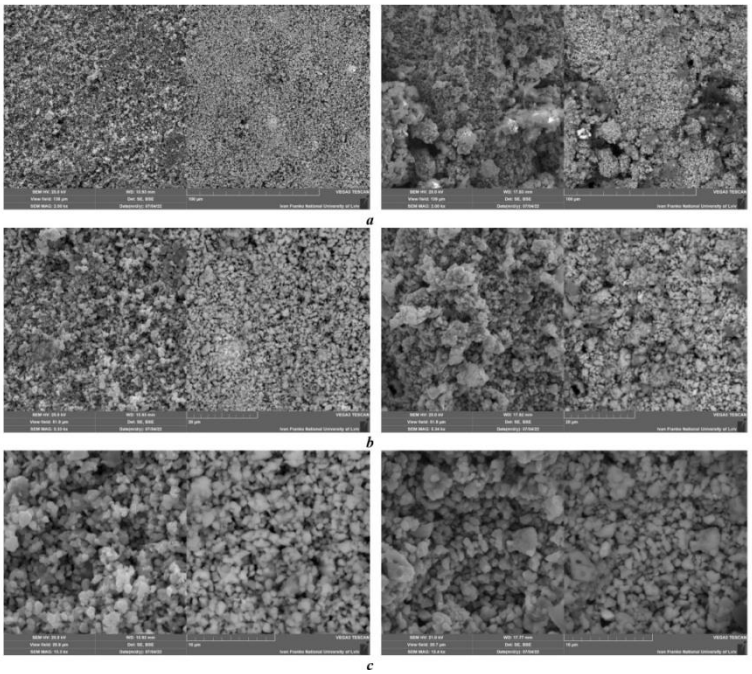

Fig. 4. SEM-images of $Pr_{0.7}Ca_{0.3}MnO_3$ before (left) and after (right) lithiation at different magnification: *a* – 2000x, *b* – 5330x, *c* – 13300x.

The composition was presented without components from electrolyte such as C, F, and P (Fig. 5). Selected charge and discharge curves for battery prototypes are presented at Fig. 6. In the case of Eu, we can see two reactions (two large plateaus on charge and discharge curves). Quantity of intercalated Li depends on volume of cathode phase. Pr-based electrodes demonstrated only one reaction of Li-insertion, whereas $Eu_{0.5}Ca_{0.5}MnO_3$-electrode showed two sequential reactions: I – Li-intercalation, II – redox and structural transformation of Eu^{2+}/Eu^{3+}cations with disproportionation of oxide phase.

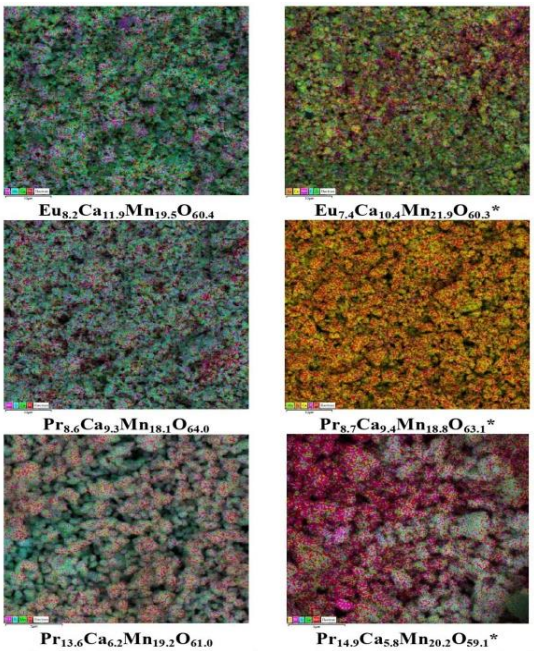

Fig. 5. Elemental mapping of the ceramics surface of the samples before (left) and after lithiation (right); * – composition without components from electrolyte: C, F, and P.

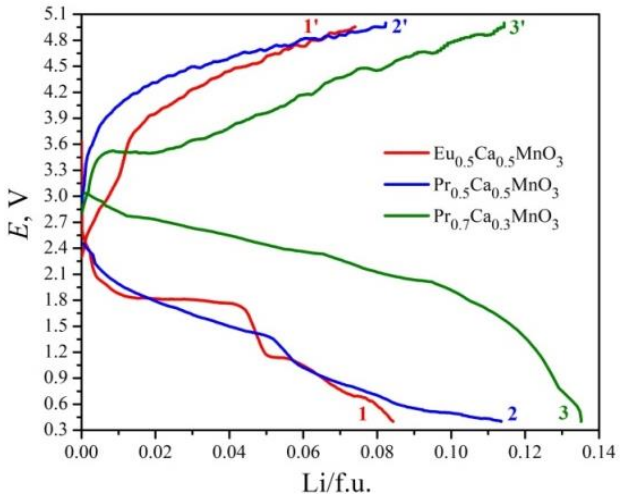

Fig. 6. Selected charge and discharge curves for battery prototype at 0.2 mA/cm^2 (1, 2, 3 – lithiation of $Eu_{0.5}Ca_{0.5}Mn_{O3}$, $Pr_{0.5}Ca_{0.5}MnO_3$, and $Pr_{0.7}Ca_{0.3}MnO_3$; 1', 2', 3' – delithiation of $Eu_{0.5}Ca_{0.5}MnO_3$, $Pr_{0.5}Ca_{0.5}MnO_3$, and $Pr_{0.7}Ca_{0.3}MnO_3$, respectively.

Formed $Li_yM_{1-x}Ca_xMnO_3$ solid solutions can be interpreted as fill-up $GdFeO_3$ orthorhombic perovskite. The insertion of lithium into the structure presumably occurs in the voids between the layers of large cations [*M*/Ca] and the layers of octahedra [MnO_6]. Under experimental conditions (Li-metal anode) we observed the formation of solid solutions with corresponding compositions: $Li_{0.084}Eu_{0.5}Ca_{0.5}MnO_3$, $Li_{0.113}Pr_{0.5}Ca_{0.5}MnO_3$, and $Li_{0.134}Pr_{0.7}Ca_{0.3}MnO_3$. For $Eu_{0.5}Ca_{0.5}MnO_3$ and $Pr_{0.5}Ca_{0.5}MnO_3$ phases lithiation occurs at the potential below 2.5 V, while for the sample with higher Pr content - at the potential < 3.0 V. Similar electrochemical behavior we already observed for $Nd_{1-x}Ca_xMnO_3$ solid solutions [25]. The electrochemical lithation of these oxide ceramics was carried out.

Intercalation of Li into structural voids of oxide phase took place during discharge process at potential below 3.5 V. The compositions of obtained Li-containing solid solutions were $Li_{0.057}Ca_{0.5}Nd_{0.5}MnO_3$, $Li_{0.091}Ca_{0.3}Nd_{0.7}MnO_3$, and $Li_{0.113}Ca_{0.05}Nd_{0.95}MnO_3$. Similarly, we noticed the formation of Li-containing aggregates with dimension of 1-3 μm. Small grains had block-like shape and diameter of < 250 nm.

Conclusions

During electrochemical lithiation of $M_{1-x}Ca_xMnO_3$ (M = Pr, Eu) ceramics (structure type $GdFeO_3$, space group *Pnma*, Pearson code *oP*20) the $Li_yM_{1-x}Ca_xMnO_3$ solid solutions of inclusion were obtained and investigated using energy-dispersive X-ray spectroscopy, X-ray fluorescence and X-ray powder diffraction methods. The unit cell parameters of initial phases correlate well with the cation radius of the rare-earth metal. X-ray phase and structural analysis of lithiated samples showed the formation of phases with increased cell volumes. Synthesized by electrochemical lithiation phases have compositions $Li_{0.084}Eu_{0.5}Ca_{0.5}MnO_3$, $Li_{0.113}Pr_{0.5}Ca_{0.5}MnO_3$, and $Li_{0.134}Pr_{0.7}Ca_{0.3}MnO_3$. In the case of Eu and Pr-containing samples the existence of amorphous halo (on the X-rays diffraction pattern) based on the by-products is explained by reaction between of oxide surface and components from electrolyte. After electrochemical lithiation the aggregates with size of 200-900 nm of block-like or irregular shape are formed.

Kordan V.M. – Ph.D, Research Fellow;
Zaremba O.I. – Ph.D, Associate Professor;
Demchenko P.Yu. – Ph.D, Senior Research Fellow;
Pavlyuk V.V. – D.Sc, Professor.

[1] P. Villars, K. Cenzual (Eds.) Pearson's Crystal Data – Crystal Structure Database for Inorganic Compounds, ASM International: Materials Park, OH, USA.Release, 2019/20.
[2] M. Yashima, R. Ali, *Structural phase transition and octahedral tilting in the calcium titanate perovskite $CaTiO_3$*, Solid State Ionics, 180, 120 (2009); https://doi.org/10.1016/j.ssi.2008.11.019.
[3] P. Wagner, G. Wackers, I. Cardinaletti, J. Manca, J. Vanacken, *From colossal magnetoresistance to solar cells: An overview on 66 years of research into perovskites*, Phys. Status Solidi A, 9, 1700394 (2017); https://doi.org/10.1002/pssa.201700394.
[4] S. Yoon, E. H. Otal, A. E. Maegli, L. Karvonen, S. K. Matam, S. Riegg, S. G. Ebbinghaus, J. C. Fallas, H. Hagemann, B. Walfort, S. Pokrant, A. Weidenkaff, *Improved photoluminescence and afterglow of CaTiO3:Pr3+ by ammonia treatment*, Opt. Mater. Express, 3(2), 248 (2013); https://doi.org/10.1364/OME.3.000248.
[5] P. Kaur, K. Singh, *Review of perovskite-structure related cathode materials for solid oxide fuel cells*, Ceram. Int, 46(5), 5521 (2020); https://doi.org/10.1016/j.ceramint.2019.11.066.
[6] M. E. Arroyo-de Dompablo, C. Krich, J. Nava-Avendaño, M. R. Palacín, F. Bardé, *In quest of cathode materials for Ca ion batteries: the $CaMO_3$ perovskites (M = Mo, Cr, Mn, Fe, Co, and Ni)*, Phys. Chem. Chem. Phys., 18,19966 (2016); https://doi.org/10.1039/C6CP03381D.
[7] A. Mai, V. A. C. Haanappel, S. Uhlenbruck, Fr. Tietz, D.Stöver, *Ferrite-based perovskites as cathode materials for anode-supported solid oxide fuel cells: Part I. Variation of composition*, Solid State Ionics, 176(15–16), 1341(2005); https://doi.org/10.1016/j.ssi.2005.03.009.
[8] J. Han, K. Zheng, K. Świerczek, *Nickel-based layered perovskite cathode materials for application in intermediate-temperature solid oxide fuel cells*, Funct. Mater. Lett., 4(2), 151 (2011); https://doi.org/10.1142/S1793604711001853.
[9] Z. Lu, Fr. Ciucci, *Anti-perovskite cathodes for lithium batteries*, J. Mater. Chem. A., 6, 5185 (2018); https://doi.org/10.1039/C7TA11074J.
[10] M. Amores, H. El-Shinawi, I. McClelland, S. R. Yeandel, P.J. Baker, R.I. Smith, H. Y. Playford, P. Goddard, S. A. Corr, E. Cussen, *$Li_{1.5}La_{1.5}MO_6$ ($M = W^{6+}$, Te^{6+}) as a new series of lithium-rich double perovskites for all-solid-state lithium-ion batteries*, J. Nat. Commun, 11, 6392 (2020); https://doi.org/10.1038/s41467-020-19815-5.
[11] J. Yan, D Wang., X. Zhang, J. Li, Q. Du, X. Liu, J. Zhang, X. Qi, *A high-entropy perovskite titanate lithium-ion battery anode*, J. Mater. Sci, 55, 6942 (2020); https://doi.org/10.1007/s10853-020-04482-0.
[12] B. Rożdżyńska-Kiełbik, I. Stetskiv, V. Pavlyuk, A. Stetskiv, *Significant improvement of electrochemical hydrogenation, corrosion protection and thermal stability of $LaNi_{4.6}Zn_{0.4-x}Lix$ ($x \leq 0.2$) solid solution phases due to Li-doping*, Solid State Sci. 113, 106552 (2021); https://doi.org/10.1016/j.solidstatesciences.2021.106552.
[13] I. Stetskiv, V. Kordan, I. Tarasiuk, V. Pavlyuk, *Synthesis, crystal structure and physical properties of the $TbCo_{4.5}Si_xLi_{0.5-x}$ solid solution*, Physics and Chemistry of Solid State, 22(3), 577 (2021); https://doi.org/10.15330/pcss.22.3.577-584.
[14] N. O. Chorna, V. M. Kordan, A. M. Mykhailevych, O. Ya. Zelinska, A. V. Zelinskiy, K. Kluziak, R. Ya. Serkiz, V. V. Pavlyuk, Electrochemical hydrogenation, lithiation and sodiation of the $GdFe_{2-x}M_X$ and $GdMn_{2-x}M_X$ intermetallics, Voprosy khimii i khimicheskoi tekhnologii, 2, 139 (2021); https://doi.org/10.32434/0321-4095-2021-135-2-139-149.

[15] A. Balińska, V. Kordan, R. Misztal, V. Pavlyuk, *Electrochemical and thermal insertion of lithium and magnesium into Zr_5Sn_3*, J. Solid State Electrochem., 19(8), 2481 (2015); https://doi.org/10.1007/s10008-015-2895-7.
[16] G. Kowalczyk, V. Kordan, A. Stetskiv, V. Pavlyuk, *Lithiation and magnesiation of R_5Sn_3 (R = Y and Gd) alloys*, Intermetallics, 70, 53 (2016); https://doi.org/10.1016/j.intermet.2015.12.004.
[17] V. Pavlyuk, W. Ciesielski, N. Pavlyuk, D. Kulawik, M. Szyrej, B. Rozdzynska-Kielbik, V. Kordan, *Electrochemical hydrogenation of $Mg_{76}Li_{12}Al_{12}$ solid solution phase*, Ionics, 25(6), 2701 (2019); https://doi.org/10.1007/s11581-018-2743-8.
[18] V. Pavlyuk, W. Ciesielski, N. Pavlyuk, D. Kulawik, G. Kowalczyk, A. Balińska, M. Szyrej, B. Rozdzynska-Kielbik, A. Folentarska, V. Kordan, *Hydrogenation and structural properties of $Mg_{100-2x}Li_xAl_x$ (x=12) limited solid solution*, Mater. Chem. Phys., 223, 503 (2019) https://doi.org/10.1016/j.matchemphys.2018.11.007.
[19] P. Solokha, S. De Negri, A. Saccone, V. Pavlyuk, B. Marciniak, J. C. Tedenac, *$Tb_2Ni_2Mg_3$: a new structure type derived from the $Ru_3Al_2B_2$ type*, Acta Crystallogr. C Struct. Chem., 63(2), i13-i1631(2007); https://doi.org/10.1107/S0108270107001503.
[20] P. Solokha, S. De Negri, V. Pavlyuk, A. Saccone, G. Fadda, *Synthesis and Crystallochemical Characterisation of the Intermetallic Phases $La(Ag_xMg_{1-x})_{12}$ ($0.11 \le x \le 0.21$), $LaAg_{4+x}Mg_{2-x}$ ($-0.15 \le x \le 1.05$) and $LaAg_{2+x}Mg_{2-x}$ ($0 < x \le 0.45$)*, Eur. J. Inorg. Chem., 30, 4811 (2012); https://doi.org/10.1002/ejic.201200700.
[21] V. V. Pavlyuk, I. M. Opainych, O. I. Bodak, T. Palasinska, B. Rozdzynska, H. Bala, *Interaction of compounds in La-Ni-Zn system*, Pol. J. Chem., 71(3), 309 (1997).
[22] A. I. Horechyy, V. V. Pavlyuk, O. I. Bodak, *X-Ray Investigation of the Ce-Cu-Cd System at 570 K*, Pol. J. Chem., 73(10), 1681 (1999).
[23] MTech. Retrieved from: http://chem.lnu.edu.ua/mtech/mtech.htm [in Ukrainian].
[24] J. Rodriguez-Carvajal, The Satellite Meeting on Powder Diffraction of the XV Congress of the IUCr (Toulouse, 1990), p. 127.
[25] V. M. Kordan, O. I. Zaremba, P. Yu. Demchenko, V. V. Pavlyuk, *Synthesis and Electrochemical Properties of $Li_yCa_xNd_{1-x}MnO_3$ Solid Solution*, Acta Phys. Pol. A., 114(4), 273 (2022); https://doi.org/10.12693/APhysPolA.141.273.

В. Кордан[1], О. Заремба[1], П. Демченко[1], В. Павлюк[1,2]

Синтез та електрохімічні властивості твердих розчинів $Li_yM_{1-x}Ca_xMnO_3$ (M = Pr, Eu)

[1]*Львівський національний університет імені Івана Франка, Львів, Україна*,
[2]*Гуманітарно-природничий університет імені Яна Длугоша, Ченстохова, Польща*, vasyl.kordan@lnu.edu.ua

Нові Li-вмісні тверді розчини $Li_yM_{1-x}Ca_xMnO_3$ (M = Pr та Eu) були синтезовані електрохімічним літіюванням керамік зі структурою перовскіту. Якісний та кількісний склад вихідних (до літіювання) та Li-вмісних керамік визначили методами скануючої електронної мікроскопії та енергодисперсійної рентгенівської спектроскопії. Співвідношення між кількостями катіонів M/Ca/Mn в складі керамік було підтверджено рентгенівською флуоресцентної спектроскопією. Кристалічну структуру твердих розчинів $M_{1-x}Ca_xMnO_3$ до літіювання (структурний тип $GdFeO_3$, просторова група *Pnma*, символ Пірсона *oP*20) та після літіювання (структура включення на основі типу $GdFeO_3$) визначити та уточнили методом Рітвельда. Рентгенівський структурний аналіз вказав на збільшення параметрів елементарної комірки для Li-вмісних фаз. Присутність аморфного гало на дифрактограмах у випадку Eu- та Pr-вмісних зразків пояснюється побічними продуктами реакції взаємодії поверхні оксидних фаз та компонентів з електроліту. За умов експерименту (анод на основі металічного Li), кількість інтеркальованого літію зростає у ряду: $Li_{0.084}Eu_{0.5}Ca_{0.5}MnO_3$, $Li_{0.113}Pr_{0.5}Ca_{0.5}MnO_3$, $Li_{0.134}Pr_{0.7}Ca_{0.3}MnO_3$. Метод скануючої електронної мікроскопії показав утворення Li-вмісних агрегатів розміром 200-900 нм. Зерна фаз демонструють блокоподібну чи нерегулярну форми із розвиненою поверхнею морфології.

Ключові слова: рентгенівська дифракція; електронна мікроскопія; структура перовскіту; електрохімічне літіювання.